THE STRAPS WITH DIFFERENT FIBER ORIENTATIONS AFFECTING THE DYNAMIC BEHAVIOR OF THE SINGLE STRAP JOINTS

Elif Unver[1], Ferhat Kadioglu[2], M. Emin Ercan[2]

[1]Turkish Aerospace Industry, Kahramankazan, Ankara, 06980, Turkey

[2]Ankara Yildirim Beyazit University, Ulus, Ankara, 06050, Turkey

ABSTRACT

In spite of many existing works related to bonding techniques of polymer composites such as Single Lap Joints (SLJs) and Double Lap Joints (DLJs), investigation about the Single Strap Joints (SSJs) is quite limited. In this study, dynamic behavior of the SSJs with the glass fiber reinforced polymer adherends and straps was evaluated using a vibrating beam technique. The effects of the straps with different stacking sequences of $\pm 45^0$ angles on the dynamic performance of the joints were investigated, and a special emphasis was given to their damping values. Two different lengths of unidirectional adherends with ten plies were used to get two different bonded (strap) lengths, 25 mm and 45 mm. On the other hand, four different types of straps were produced - each with ten plies; three types consisted of eight of plies of 0^0 fiber angle and two plies of $\pm 45^0$ angles at the top, at the bottom and in the middle of the straps, and the remaining one with ten plies of 0^0 angle. The dynamic measurements were made at the fundamental natural frequency of the specimens with fixed-free boundary conditions. The results showed that the straps that consisted of the plies with the $\pm 45^0$ angles contributed to the joint damping performance considerably, compared to those with the only 0^0 angle. A numerical modal analysis was also conducted using a commercial package program. The predicted and experimental results were found in an agreement.

Keywords: Bonded Single Strap Joints, Modal Analysis, Finite Element, Composite Materials

Corresponding author: Prof. Dr. Ferhat KADIOGLU (ferkadioglu@gmail.com)

[1] Senior Manufacturing Engineering
[2] Prof. Dr., Aviation and Aerospace Engineering

1. INTRODUCTION

Polymer matrix composites with fiber reinforcement are demanded by especially automotive and aerospace industries due to their desired properties such as high strength/stiffness, low density and high resistance to the corrosion and fatigue problems. Some traditional joining techniques such as bolted or riveted joints for these materials have been used for many years [1-2], however, existence of hole in the composite adherends causes stress concentrations leading to a poor joint performance. On the other hand, adhesively-bonded joints are found feasible for assembling these materials as these joints provide relatively uniform stress distributions and continuity in the bonded region resulting in relatively higher joint performance. Some works related to the subject have been reviewed by the current author [3]. For example, Mathews and Tester [4] investigated the influence of stacking sequence on the strength of bonded carbon fiber reinforced polymer single lap joints (SLJs). It was found that both lay-up and stacking sequence influenced the joint strength. In another work [5], a three-dimensional (3-D) Finite Element Model (FEM) was developed to investigate the effect of geometry on the strength of SLJs with the adherends of composite laminates under tensile loading. As an important joining technique, the most critical parts of the adhesively bonded joints subjected to the tensile loading are the ends of the overlap (bonded) region where the normal stresses cause high concentrations leading to a poor performance. To overcome this, some attempts have been made by modifying shape of the bonded region in which the adhesive layer would be able to experience the compression stresses rather than the peeling. Razavi et al. [6] studied numerically and experimentally the role of sinusoid interface shape on the stress distribution and load bearing capacity of the adhesively-bonded SLJs. Some parametric studies were conducted using the FEM to investigate the role of various wave heights, wave lengths, adhesive thicknesses and also mechanical properties of adhesives and adherends on the stress distributions of the bonded joints. It was found that existence of local compressive stresses at both ends of adhesive layer in sinusoid joints with negative bond slope improved the joints strength. In a similar work [7], the role of adhesive–adherend interface morphology on the mechanical behavior of adhesively-bonded lap joints was studied. Two mirror-image types of joints with a zigzag interface containing 'positive and negative' interlocking teeth were fabricated and their tensile behavior was measured and compared to the response of a standard flat joint. The conducted numerical analysis suggested that the stress distribution along the bond line and thus the initial fracture load of the joint was altered considerably by the positive and negative interlocking teeth. The tendency of a crack to either propagate along the bond or to arrest also depended strongly on morphological details. When crack arrested, the bonded joint could sustain a higher load and thus benefited from some of the intrinsic properties of the adherends (e.g. the plasticity of metal adherends) to enhance energy absorption and toughness. Also, a series of experiments and detailed numerical simulations were carried out to study the performance of SLJs with non-flat interfaces loaded at a small angle to the mean bond plane [8]. In the experimental part, composite adherends with sinusoidal bonding surfaces were fabricated in a purpose-built mould. SLJs with a flat interface were also manufactured using the same composite material and with the same overall shape. The experiments showed that the interface non-flatness has significant effect on the mechanical behavior and strength of the bonded joints. In another work, Avila and Bueno [9] studied experimental and numerical analysis of a

novel design of the SLJ, called 'wavy-lap joint'. The results showed an average increase of nearly 41% on loading, which was attributed to the compressive stress field developed inside the wavy-lap joint. Nearly the same conclusion was made by Fessel et al. [10] who compared the stress distribution of the 'reverse-bent' and the 'wavy joint', with the stresses of the traditional lap-shear joint, when using the FEM. A parametric study was carried out showing trends influencing stresses in the adhesive layer. The strength of 'reverse-bent' joints was found to be up to 40% higher compared to flat joints using various substrate materials, adhesives and overlap lengths. In spite of numerous more works related to the SLJs, a Single Strap Joint (SSJ) with its practical application is believed to be another option.

In spite of many studies about the different types of bonded joints, there is a lack of motivation about the SSJs. For the current work, an investigation of the SSJs is aimed using a vibrating beam test with fixed-free end conditions. Numerical modal analysis of the joints were also conducted to find out their natural frequencies and mode shapes. In studying these joints, the main motivation was given to the values of damping and flexural rigidity, which were found at the natural frequency of the specimens used. All the adherends were prepared with totally ten unidirectional (0^0) plies. Two different lengths of adherends were used, 101 mm and 111 mm. On the other hand, different types of straps with different stacking sequences of $\pm 45^0$ fiber angles were produced (see Figure 1); S1- the one with totally ten 0° angle plies, S2- the one with eight plies of 0° and two plies of 45° located in the middle of the strap (-45^0 in the fifth and $+45^0$ sixth layer), S3- the one with eight plies of 0° and two plies of 45° located on the outer surface of the strap (-45^0 in the ninth and $+45^0$ tenth layer), and S4- the one with eight plies of 0° and two plies of 45° located in the inner surface of the strap close to the adhesive layer (-45^0 in the first and $+45^0$ second layer). After proper surface preparation of the components to be bonded, an adhesive film, AF 163-2K produced by 3M, was used to prepare the joints.

2. EXPERIMENTATION

2.1. Manufacturing of the Joints

All the adherends were extracted from the ten plies of glass fiber reinforced laminates, Hexply 913/33%/UD280, produced by Hexcel, which were cured in an autoclave under a temperature range of 120-180 ^{0}C and pressure of about 5 bars, with 0.5-3.5 ^{0}C/min heat-up rates [11]. The adherends were machined from the cured plates, in the dimensions of two different lengths (101 mm and 111 mm), a thickness of 2.32 mm and a width of 25 mm. While the shorter adherends were used for the joints with 25 mm strap length, the longer ones for those with 45 mm length. First, surface preparation of the adherends to be bonded was made using peel-ply removal as the sole surface preparation technique, then an adhesive film, AF163-2K, produced by 3M, was applied to these surfaces at room temperature. After all, the specimens were put in an autoclave to cure the adhesive layer and to get the bonded joints, which were subjected to a temperature of 120 ^{0}C and 3 bars of pressure for 90 minutes [12]. The actual dimensions and weight of the joints are

presented in Table 1. The equivalent thickness and density of the joints have been measured from their known data. The manufactured specimens with different strap lengths are show in Figure 2.

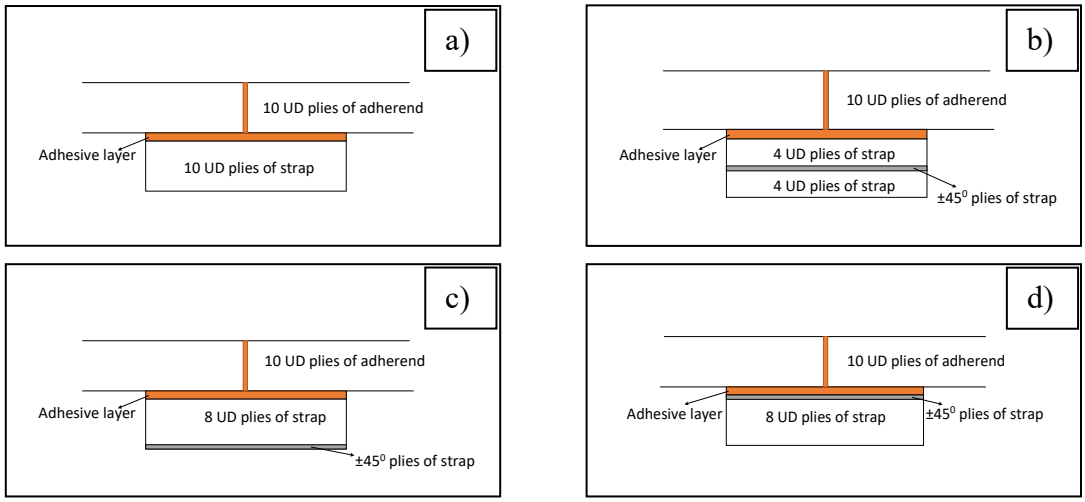

Figure 1. A representation of the specimens with different types of straps; a) S1, b) S2, c) S3, and d) S4

Table 1. The measurements of the specimens used

Length of Adherends (mm)	Length of Straps (mm)	Equiv. thickness of the SSJ (mm)	Width of the SSJ (mm)	Mass of the SSJ (gr)	Equiv. Density of the SSJ (kg/m^3)
101	25	2.81	25	23.91	1794.95
111	45	2.81	25	28.00	1794.95

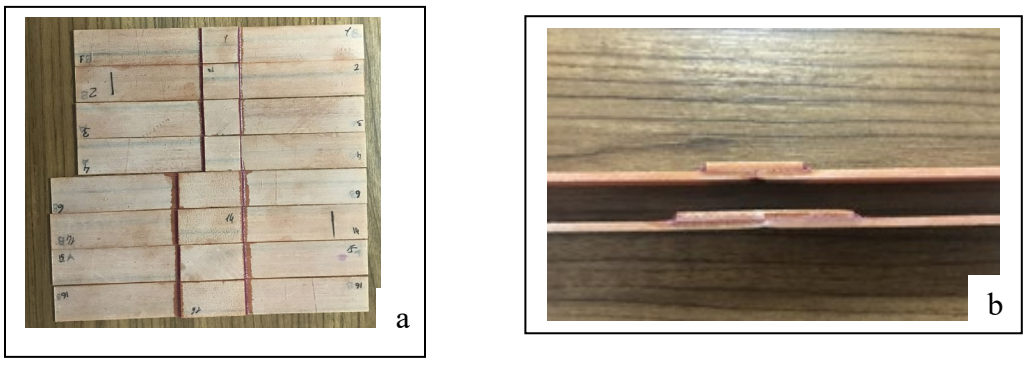

Figure 2. a) Manufactured Single Strap Joints (SSJs) with different adherend and strap lengths**,**

b) Side view of SSJs with 25 mm and 45 mm length of straps

2.2. The Test Set-up

For the dynamic measurements of the specimens, a vibrating beam test set-up shown in Figure 3 was used. The experimental set-up includes an instrumented impact hammer (8206 Bruel & Kjaer) to generate impulse, and a non-contact microphone (Type 1706/8206 Bruel & Kjaer) to pick up the response from the specimen. The impacted specimen is aimed to give its natural frequencies within a required frequency domain, via some distinguished peak values of the amplitude, depending on the mode shapes. A sophisticated data acquisition card (HBM QuantumX MX410B) was used to collect the digital values from the hammer and microphone. The set-up is supported by a software (HBM Catman data acquisition software) to process the data according to the required output format for visualization and analysis. The natural frequency, flexural rigidity and damping values of the specimens can be measured easily via this technique. For the damping values, the half power bandwidth method was used, and more details about the method are explained below. It is important to note that the specimens were placed into the fixed support properly and the clamped part was tightened firmly, which was crucial for reliable measurements. For each category of the specimens, two different specimens were tested to see if repeatable experimental results were obtained, and average results with percentage deviation were presented. All the tests were conducted under a controlled environment, 23 ^{0}C and 50% relative humidity.

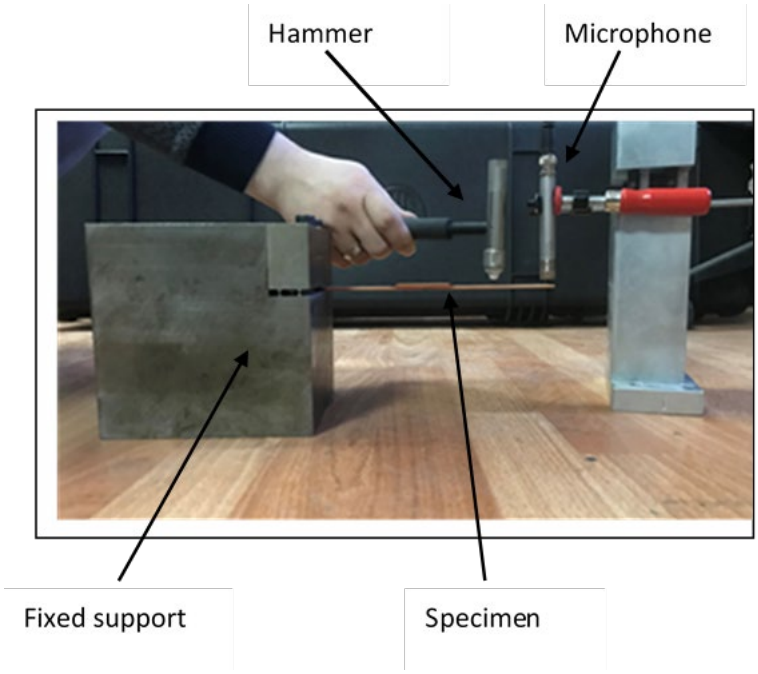

Figure 3. The experimental test set-up with fixed-free boundary conditions

2.3. Dynamic Measurements

The resonant frequency of a beam that is a function of its elastic modulus, dimensions and density is found using Equation (1) [13].

$$f_n = \frac{1}{2\pi}\left(\frac{\lambda_n}{l}\right)^2 \sqrt{\frac{EI}{\rho t b}} \tag{1}$$

where;

λ_n = 1.875 is the 1st eigenvalue for clamped-free end conditions

n is the mode number

E is the flexural modulus,

I is the second moment of area

l is the length of the beam

ρ is the mass density

t is the thickness

b is the width of the beam

EI is the flexural rigidity

For this study, the half-power bandwidth method was used to obtain the damping value. The method suggests that frequency and amplitude values be determined using Figure 4. The half-power bandwidth is (f_2-f_1) reached at f_n, the resonant frequency, where f_1, f_2 are the frequency points selected on the curve at the maximum amplitude multiplied by $1/\sqrt{2}$. The loss factor, η, can be calculated using equation (2).

$$\eta = \frac{f_2 - f_1}{f_n} \tag{2}$$

For convenience, damping is usually presented in Specific Damping Capacity (SDC), ψ, which is defined as the ratio of the energy dissipated per cycle to the maximum elastic energy stored per cycle, per unit volume. This ratio is usually expressed as a percentage. For small damping values, it is known there is a relationship between η and ψ [14], presented in equation (3)

$$\psi = 2\pi\eta \tag{3}$$

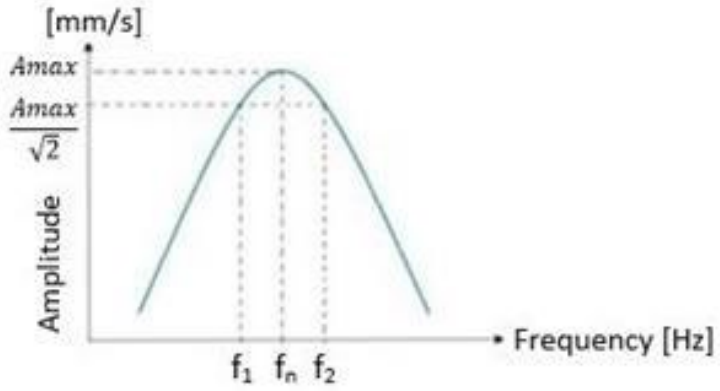

Figure 4. Schematic representations of the definitions of the half-power bandwidth method

2.4. Numerical Modal Analysis

A numerical modal analysis of the SSJs with fixed-free boundary conditions was conducted using the Finite Element Analysis through ABAQUS package program. A three dimensional (3-D) meshed model of the joint is presented in Figure 5. For the adhesive layer, the element type used was C3D8R that is an 8-node linear brick, reduced integration with hourglass control. The element type used for the adherends and straps was SC8R that is an 8-node quadrilateral in-plane general-purpose continuum shell, reduced integration with hourglass control, finite membrane strains. Natural frequencies, mode shapes and flexural rigidity of the joints were predicted and compared with the experimental results. Note that only the fundamental (first) frequency was used for the comparison reasons.

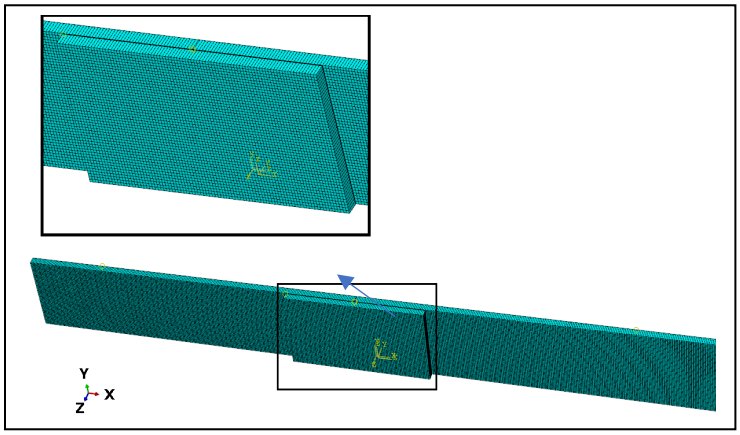

Figure 5. A 3-D meshed model of the Single Strap Joint (SSJ)

The input data for the numerical modal analysis are shown in Table 2, where E denotes flexural modulus, G, shear modulus, E_1 denotes modulus of elasticity in longitudinal direction, also defined as the fiber direction, E_2 for modulus of elasticity in lateral direction, G_{12} is in-plane shear modulus, G_{13} is transverse shear modulus in 2-3 plane, G_{23} is transverse shear modulus in 2-3 plane. υ denotes Poisson's ratio, and ρ is mass density for both isotropic and orthotropic materials.

Table 2. Input data used for the numerical modal analysis

Materials	E_1 (MPa)	E_2=E_3 (MPa)	G_{12}= G_{13} (MPa)	G_{23} (MPa)	υ_{12}= υ_{12}= υ_{23}	ρ (kg/m^3)
Laminate Hexply 913/33%	44000	13000	6900	6300	0.27	1800
Adhesive Film (AF163-2K)	2000	-	-	-	0.34	1100

3. RESULTS AND DISCUSSION

Different stacking sequences of the $\pm45^0$ angle plies at different locations in the straps were found to have considerable effects on the dynamic values of the Single Strap Joints (SSJ). The $\pm45^0$ angle plies enhanced the damping performance of the joints considerably, while their effects in terms of flexural rigidity (*EI*) were limited, compared to the joints with the only 0^0 angle plies of the straps (S1). The experimental values of the fundamental natural frequency, the equivalent flexural rigidity and the specific damping capacity (SDC) of the specimens are presented in Table 3. It is worth pointing out that the average experimental results of two specimens for each category were put in the table, and that deviation of each was not bigger that 1%.

The maximum values of the frequency and flexural rigidity are belonging to the joints with 25 mm length of straps with the 0^0 angle (S1), about 57.15 Hz and 3.20 Pa.m^4, respectively. These values are 47.22 Hz and 2.18 Pa.m^4 for those with the 45 mm strap lengths, respectively. The value of the SDC for these specimens is about 3.30%, a minimum, compared to the others (S2, S3 and S4). On the other hand, the specimens with the $\pm45^0$ angle plies of the straps have relatively lower values of the natural frequency and flexural rigidity, about 56 Hz and 3.10, respectively, but quite considerable higher damping values, 7.39%, 8.12% and 7.63 for the S2, S3 and S4 for the joints with 25 mm strap length, respectively. In this case, the increase in the damping value is about 130%, while the decrease in the value of flexural rigidity is only about 3.43%. It seems the joints with the 45 mm strap length has lower values of the frequency and flexural rigidity but a very small increase in the damping value if compared to those with the 25 mm strap length. The increase in the damping value is about 5.5% but the decrease in the flexural rigidity is about 35% in average. It is believed that the rigidity decrement is due to the relatively longer length of the joints with the 45 mm strap (222 mm), compared to those with the 25 mm strap length (202 mm), while they both have the same amount of thickness. Figure 6 indicates the first, second and third mode shapes of the SSJs with their predicted natural frequencies. The figure is a representative predicted shape to

the joints with 25 mm and 45 mm strap lengths. Note that only first predicted natural frequencies were used and compared with the experimental ones presented in Table 3. Figure 7 shows two representative experimental outputs obtained through the software used.

Table 3. A comparison of experimental (Exp.) and predicted (Pred.) results

Specimens	Strap Length (mm)	Exp. NF* f_n (Hz)	Pred. NF* f_n (Hz)	Exp. FR* EI (Pa.m^4)	Pred. FR* EI (Pa.m^4)	Exp. SDC* (%)
S1	25	57.15	60.40	3.20	3.57	3.33
S2	25	56.20	60.38	3.09	3.57	7.39
S3	25	56.32	60.39	3.10	3.57	8.12
S4	25	55.88	60.35	3.06	3.56	7.63
S1	45	47.22	49.30	2.18	2.38	3.25
S2	45	46.94	49.27	2.16	2.38	8.26
S3	45	47.11	49.29	2.17	2.38	7.88
S4	45	46.81	49.23	2.14	2.37	8.21

* NF: Natural Frequency, FR: Flexural Rigidity, SDC: Specific Damping Capacity

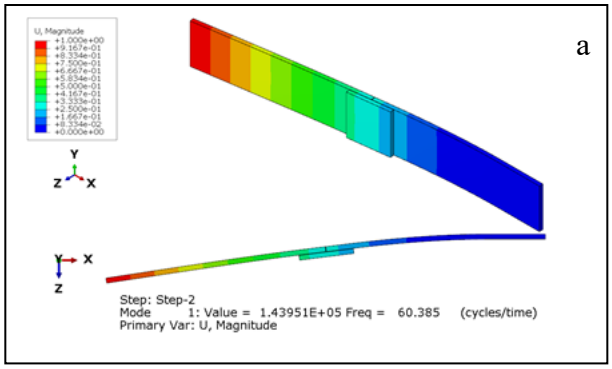

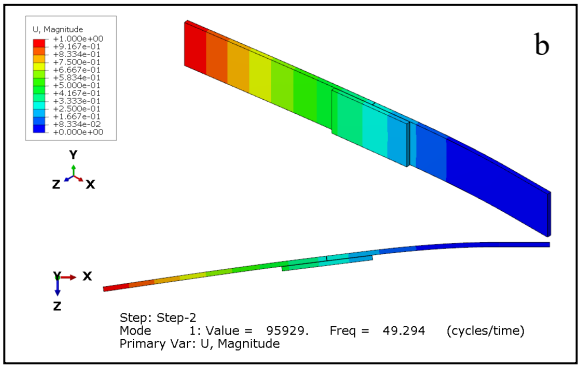

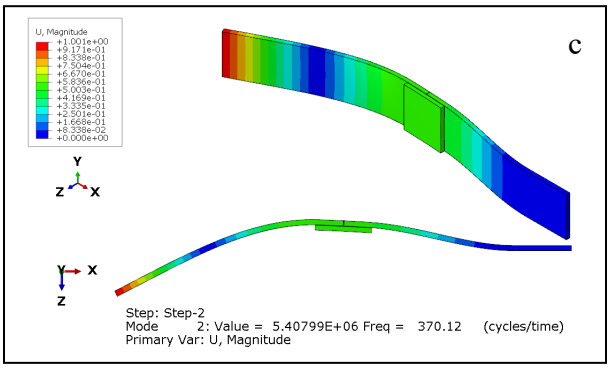

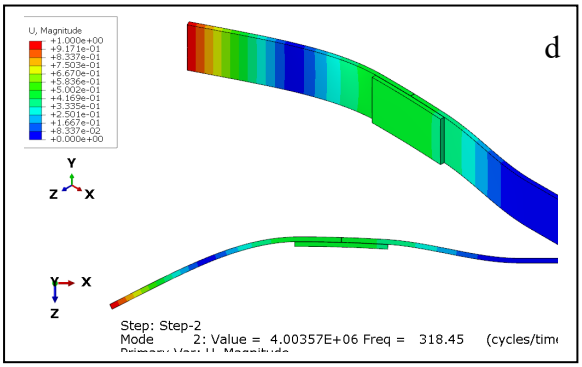

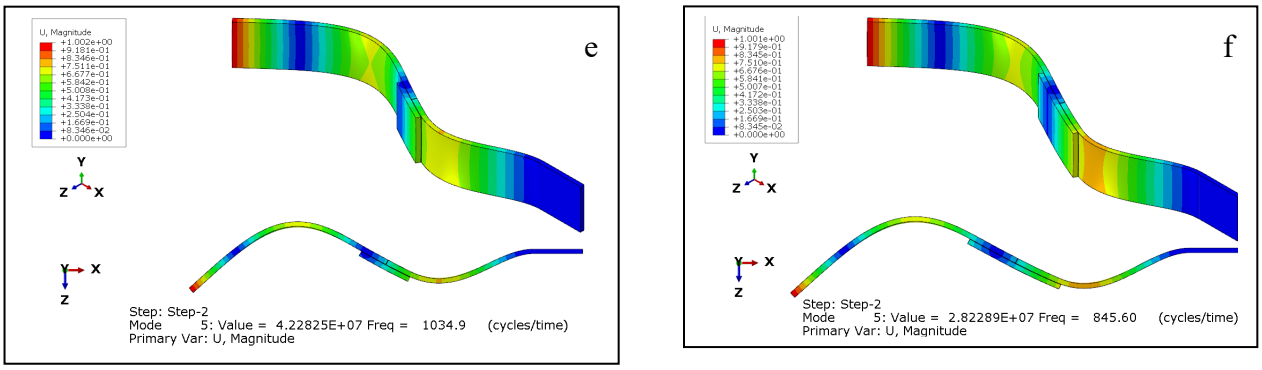

Figure 6. a, b) first, **c, d)** second, and **e, f)** third mode shapes of the SSJs with 25 mm and 45 mm strap lengths, respectively.

This work proves that it is possible to increase the damping performance of adhesively bonded joints by shifting some parameters that do not compromise the flexural rigidity too much. In the case of the SSJs, inclusion of $\pm 45^0$ plies into the strap laminates have enhanced the damping performance considerably. It is worth pointing that structural damping is seen as important parameter for the design of vehicles and machines where their safety is of concern as excessive vibrations could damage their electronic components and other delicate parts.

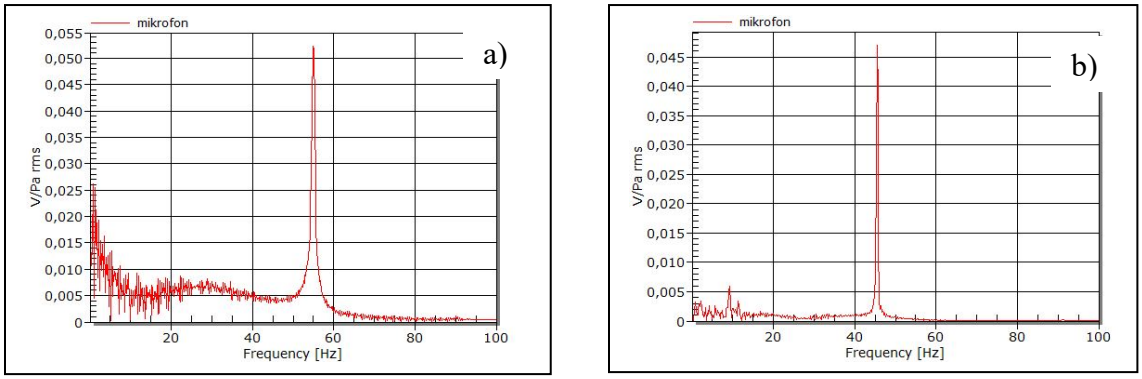

Figure 7. Two representative outputs from the vibrating beam test set-up with fixed-free boundary conditions; **a)** the SSJ with 25 mm strap length, **b)** the SSJ with 45 mm strap length

4. CONCLUSIONS

Effects of the straps mentioned above on the dynamic performance of the Single Strap Joints (SSJs) were studied. It seems the straps with $\pm 45^0$ angle plies in the different stacking sequences are able to enhance the damping performance of the joints, compared to those with the unidirectional (0^0 angle) ones. While only a small amount of decrease was found in the values of flexural rigidity, the damping values increased about 125% for the joints with the straps consisting of $\pm 45^0$ angle plies. Contribution of the longer straps (45 mm) to the damping performance of the joints was negligible, although a small decrease was observed in the value of the flexural rigidity, compared to the those with the shorter straps (25 mm).

Acknowledgments

We would like to thank to the Turkish Aerospace Industry for supporting the current work.

5. REFERENCES

[1] Chandra R, Singh SP, Gupta K, A study of damping in fiber-reinforced composites, Journal of Sound and Vibration, 2003, 262: 475-496.

[2] Li Y, Cai S, Huang X, Multi-scaled enhancement of damping property for carbon fiber reinforced composites, Composites Science and Technology, 2017, 146: 1-9

[3] Kadioglu F, Effects of compressive applied load on the adhesive single lap joint with different parameters, Journal of Adhesion, https://doi.org/10.1080/00218464.2020.1834390.

[4] Matthews FL, Tester TT, The influence of stacking sequence on the strength of bonded CFRP single lap joints, International Journal of Adhesion and Adhesives, 1985, 5(1): 13-18. https://doi.org/10.1016/0143-7496(85)90040-5

[5] Moya-Sanz EM, Ivañez I, Garcia-Castillo SK, Effect of the geometry in the strength of single-lap adhesive joints of composite laminates under uniaxial tensile load, International Journal of Adhesion and Adhesives, 2017, 72: 23-29.

[6] Razavi SMJ, Berto F, Peron M, Torgersen J, Parametric study of adhesive joints with non-flat sinusoid interfaces, Theoretical and Applied Fracture Mechanics, 2018, 93:44–55.

[7] Haghpanah B, Chiu S, Vaziri A, Adhesively bonded lap joints with extreme interface geometry, International Journal of Adhesion and Adhesives, 2014, 48:130-138.

[8] Ashrafi M, Ajdari A, Rahbar N, Papadopoulos J, Nayeb-Hashemi H, Vaziri A, Adhesively bonded single lap joints with non-flat interfaces, International Journal of Adhesion and Adhesives, 2012, 32:46–52.

[9] Avila AF, Bueno PO, Stress analysis on a wavy-lap bonded joint for composites, International Journal of Adhesion and Adhesives, 2004, 24:407–414.

[10] Fessel G, Broughton JG, Fellows NA, Durodola JF, Hutchinson AR, Evaluation of different lap shear joint geometries for automotive applications, International Journal of Adhesion and Adhesives, 2007, 27:574-583.

[11] www.hexcel.com/Resources/DataSheets/Prepreg.

[12] www.3m.com/3M/en_US/company-us/all-3m-products/~/3M-Scotch-Weld-Structural-Adhesive-Film-AF-163-2.

[13] Den Hartog JP, Mechanical Vibrations, McGraw-Hill Book Company Inc, New York, London, 1947.

[14] Singh MM, Dynamic properties of fibre reinforced polymers exposed to aqueous conditions, Department of Mechanical Engineering, University of Bristol, 1993.